J. Fluid Mech. (1995), *vol.* 289, *pp.* 141–157

A simple representation of a developing contaminant concentration field

By B. L. SAWFORD[1] AND P. J. SULLIVAN[2]

[1] CSIRO Division of Atmospheric Research, Private Bag No 1, Mordialloc, Vic. 3195, Australia

[2] Department of Applied Mathematics, University of Western Ontario, London, Ontario, Canada N6A5B9

(Received 2 December 1993 and in revised form 1 November 1994)

Chatwin & Sullivan (1990) have demonstrated that, for a wide range of self-similar scalar fields, the moments of the probability density function of concentration have a very simple form. Here, an extension to this simple form which takes account of the source distribution is developed. This extension has two effects. Firstly it modifies the values of the two parameters appearing in the original theory and in particular explains the observed behaviour of these parameters very near to a line source of heat in grid tubulence. Secondly, it introduces an additional parameter in the description of each moment beyond the second. It is shown that these additional parameters are necessary in order to describe measurements of the first four central moments throughout the concentration field from a continuous line source of heat in grid-generated turbulence.

1. Introduction

Contaminant concentration values in a turbulent flow are reduced through molecular diffusion and these changes are readily observed through the probability density function $p(\theta; \boldsymbol{x}, t)$, where

$$p(\theta; \boldsymbol{x}, t)\,\mathrm{d}\theta = \mathrm{prob}\{\theta \leqslant \Gamma(\boldsymbol{x}, t) < \theta + \mathrm{d}\theta\}, \tag{1}$$

and $\Gamma(\boldsymbol{x}, t)$ is the concentration at the position located by vector $\boldsymbol{x}$ at time t. It is generally expected (see Derksen & Sullivan 1990) that a good approximation to $p(\theta; \boldsymbol{x}, t)$ can be found by inverting the lower-order moments,

$$\overline{c^n}(\boldsymbol{x}, t) = \int_0^\infty (\theta - C)^n p(\theta; \boldsymbol{x}, t)\,\mathrm{d}\theta, \tag{2}$$

where

$$C(\boldsymbol{x}, t) = \int_0^\infty \theta p(\theta; \boldsymbol{x}, t)\,\mathrm{d}\theta, \tag{3}$$

using a maximum entropy formulation, for example. In (2) and (3), we have used C to denote the mean concentration, the fluctuating component is denoted by c, and $\Gamma = C + c$.

In Chatwin & Sullivan (1990) the simple algebraic expression,

$$\overline{c^n}(\eta) = \frac{\beta^n}{\alpha} C_0^n \{\chi(\eta)(\alpha - \chi(\eta))^n + (-1)^n (\alpha - \chi(\eta))\,\chi^n(\eta)\} \tag{4}$$

was proposed for the moments at large downstream distances in self-similar turbulent

shear flows. In (4) $\chi(\eta) = C(\eta)/C_0$, $\eta = y/L$, with similarity length scale L, and y is the cross-stream distance measured from the location of the maximum value of mean concentration $C_0 = C(0)$. The parameters α and β are constants that depend on the particular source and flow configuration. Data from a wide variety of these flows are in agreement with the proposal that $1 < \alpha < 2$ and $0.3 < \beta < 1$.

The rationale used in the derivation of (4) is that molecular diffusion acts slowly and the effects of molecular diffusion take a much greater downstream distance to develop than do the effects of turbulent convective motion. The effects of molecular diffusion can thus be approximated by modifications to the moment distribution for zero diffusivity ($\kappa = 0$) which is known exactly. In particular, the source concentration in this moment distribution is replaced by a 'local' value, αC_0, and a constant of proportionality β^n is introduced to account for the increased background concentration due to molecular diffusion.

The attraction of results like (4) is their simplicity and their ability to estimate higher moments (and hence the probability density function) given a knowledge of the mean concentration. For example, it can be shown (Derksen, Sullivan & Yip 1994) that (4) corresponds to a probability density function consisting of two delta functions. Unlike the hypothetical situation when $\kappa = 0$, the location of these delta functions corresponds to high and low (but non-zero) concentrations which are functions of η. Thus the probability density function corresponding to (4) is non-trivially different from the $\kappa = 0$ case. The moment distributions developed later in this paper do not, upon inversion, result in a probability density function consisting of two delta functions.

The disparity between convective and molecular diffusive scales is also likely to be satisfied in many regions where contaminant distributions are not self-similar and, provided α and β are taken to vary with time or with downstream distance, (4) would describe the lateral distribution of moments. There is some support for this contention based on the measured distributions of second moments. The data of Stapountzis *et al.* (1986) and Warhaft (1984) for a heated line source and of Sullivan (1971) for relative diffusion in a meandering plume in Lake Huron are considered in Moseley (1991), the data of Fackrell & Robins (1982) for an elevated point source in a turbulent boundary layer are examined in Sullivan & Yip (1989) and the Karnik & Tavoularis (1989) measurements of a line source in uniformly sheared turbulent flow are studied in Chatwin, Sullivan & Yip (1990). These data are all reasonably represented by the suggested modification to (4). This preliminary evidence has motivated the present more complete study of the lower-order moments throughout the plume from a heated line source in grid turbulence.

The theory (4) (and its proposed extension to non-self-similar scalar fields) was developed for a uniform source for which the concentration takes a fixed value θ_0 within the source fluid and is zero outside the source. Then the parameters α and β approach unity at the source. However, the data sets referred to above (and the data discussed in the present work) do not show this behaviour. This is not surprising since it is well-known that concentration statistics depend on the source details, especially in the near field (see e.g. Chatwin & Sullivan 1979; Fackrell & Robins 1982).

Here therefore we have relaxed the assumption of a uniform source distribution in order to explore its effect on the theory. Some of our asymptotic results do not require detailed assumptions about the nature of the flow (in common with the original theory). However, we also derive some results specifically for homogeneous turbulence. We do this mainly to explore the near field, where the detailed structure of the scalar field depends sensitively on the source distribution. We compare the predictions of the modified theory with detailed measurements of the first four moments of the

concentration field downstream of a line source in grid turbulence. Our objective is not to develop a complete new theory valid under arbitrary conditions, but to examine the potential limitations of the existing theory using the specific example of homogeneous turbulence.

The plan of the paper is as follows. In §2 the theory is developed for an instantaneous, arbitrary source distribution. Results for the $\kappa = 0$ case (which is generally a good approximation for small times) are derived and modified to account for the effects of molecular diffusion as was done in Chatwin & Sullivan (1990). Emphasis is placed on the contrast between uniform and non-uniform source results. A Gaussian source in homogeneous turbulence is used to illustrate the small-time behaviour. Overall, a structure for the moments that is similar to (4) is obtained but each moment higher than the second introduces a new function which we denote by $\lambda_n(t)$. In §3 the present data set is described and compared with the results of §2. Our conclusions are presented in §4.

2. Theory

2.1. *Uniform and non-uniform source results for* $\kappa = 0$

When $\kappa = 0$ the probability density function for the concentration from a uniform source of concentration θ_0 is

$$p(\theta; x, t) = \pi(x, t)\,\delta(\theta - \theta_0) + (1 - \pi(x, t))\,\delta(\theta) \tag{5}$$

where $\pi(x, t)$ is the probability of being in source fluid (see Chatwin & Sullivan 1990). The moments of p are

$$\left.\begin{aligned} C(x,t) &= \theta_0\,\pi(x,t), \\ \overline{c^2}(x,t) &= C(x,t)(\theta_0 - C(x,t)), \\ \overline{c^3}(x,t) &= C(x,t)(\theta_0^2 - 3\theta_0\,C(x,t) + 2C^2(x,t)), \\ \overline{c^4}(x,t) &= C(x,t)(\theta_0^3 - 4\theta_0^2\,C(x,t) + 6\theta_0\,C^2(x,t) - 3C^3(x,t)), \end{aligned}\right\} \tag{6}$$

Although these results apply specifically for the case of the uniform source distribution, in other respects they are very general, assuming nothing, for instance, about the nature of the flow or source configuration.

The original Chatwin & Sullivan theory (4) results from modifications to (6) to account for the effects of molecular diffusion. Specifically, θ_0 in (6) is replaced by the 'local' concentration value αC_0 and a separate factor β is used to account for other aspects of the dissipation of scalar fluctuations and instrument smoothing. It was suggested by Chatwin & Sullivan (1987) that α would be reasonably insensitive, and β would be sensitive, to instrument smoothing. Some support for this position is found in the measurements of Sakai *et al.* (Chatwin & Sullivan 1993) where four probes with sample length ranging from 0.1 to 0.5 mm were used to measure second central moments of a passive scalar concentration in a turbulent water jet. They confirmed (4) with $n = 2$ for all probe sizes and their results show the values of α to be virtually constant (a maximum and irregular variation of 4% about the mean value 1.29), while the values of β systematically increased from 0.40 to 0.57 with decreasing probe size. The effect of sampling on the present experimental data is discussed in §3.

We consider now the case in which a quantity Q of contaminant with concentration

$\mathscr{S}(x)$ is released at $t = 0$. For this non-uniform source concentration the probability density function of the concentration for $\kappa = 0$ is

$$p(\theta; x, t) = \int_{a.s.} \delta(\theta - \mathscr{S}(x'))\, P(x'; x, t)\, \mathrm{d}x', \tag{7}$$

where $P(x'; x, t)\,\mathrm{d}x'$ is the probability that fluid located by vector x at t came from a volume element $\mathrm{d}x'$ about x' at $t = 0$. The a.s. designation indicates integration over all space.

If the source volume, V_0, is finite, i.e. $\mathscr{S}(x) = 0$ for $x \notin V_0$, then the initial location of a fluid particle within the source is 'forgotten' (for a passive scalar contaminant) for times for which $\sigma_p^3(t) \gg V_0$, where $\sigma_p(t)$ is the standard deviation of the displacement of particles from a point. Then the integral in (7) decouples to give

$$p(\theta; x, t) \approx \pi(x, t)\, V_0^{-1} \int_{V_0} \delta(\theta - \mathscr{S}(x'))\, \mathrm{d}x' + (1 - \pi(x, t))\, \delta(\theta), \tag{8}$$

where the relationship

$$\pi(x, t) = \int_{V_0} P(x'; x, t)\, \mathrm{d}x' \approx V_0\, P(\mathbf{0}; x, t) \tag{9}$$

has been used to facilitate comparison with (5) and, for example, with the structure given in Chatwin & Sullivan (1989). The moments corresponding to (8) are

$$\left.\begin{aligned} \overline{c^2}(x, t) &= C(x, t)(\lambda_2 \theta_0 - C(x, t)), \\ \overline{c^3}(x, t) &= C(x, t)(\lambda_3^2 \theta_0^2 - 3\lambda_2 \theta_0\, C(x, t) + 2C^2(x, t)), \\ \overline{c^4}(x, t) &= C(x, t)(\lambda_4^3 \theta_0^3 - 4\lambda_3^2 \theta_0^2\, C(x, t) + 6\lambda_2 \theta_0\, C^2(x, t) - 3C^3(x, t)), \\ &\vdots \end{aligned}\right\} \tag{10}$$

where

$$\lambda_n^{n-1} \theta_0^{n-1} = \int_{a.s.} \mathscr{S}^n(x')\, \mathrm{d}x' \Big/ \int_{a.s.} \mathscr{S}(x')\, \mathrm{d}x' \quad (n \geqslant 2). \tag{11}$$

Without loss of generality, the source concentration scale θ_0 can be chosen so that $\lambda_2 = 1$.

Although (8) and (10) have been derived for a strictly finite source volume, the moment equations (10) with (11) also hold (provided the integrals exist) for an arbitrary source with concentration scale θ_0 and a finite representative length scale,

$$L_0 \sim \left(\theta_0^{-1} \int_{a.s.} \mathscr{S}(x)\, \mathrm{d}x\right)^{-1/3} = (Q/\theta_0)^{-1/3},$$

for times such that $\sigma_p(t) \gg L_0$. For example, (10) holds for a Gaussian source distribution.

The simple structure of higher moments given in (6) for a uniform source is recovered in (10) for a distributed source once the cloud size is much larger than the source size but with the introduction of one additional constant λ_n for each moment higher than the second. Of course, for $\mathscr{S}(x)$ uniform over V_0 in (11), $\lambda_n = 1$ and (6) is recovered from (10). The primary concern in this paper is the evolution of moments with distance downstream from the source to an asymptotic state like that given in (4) for self-similar flows. In particular, the significance of the new parameters λ_n arising from a distributed source when $\kappa \neq 0$ needs to be assessed with experimental data.

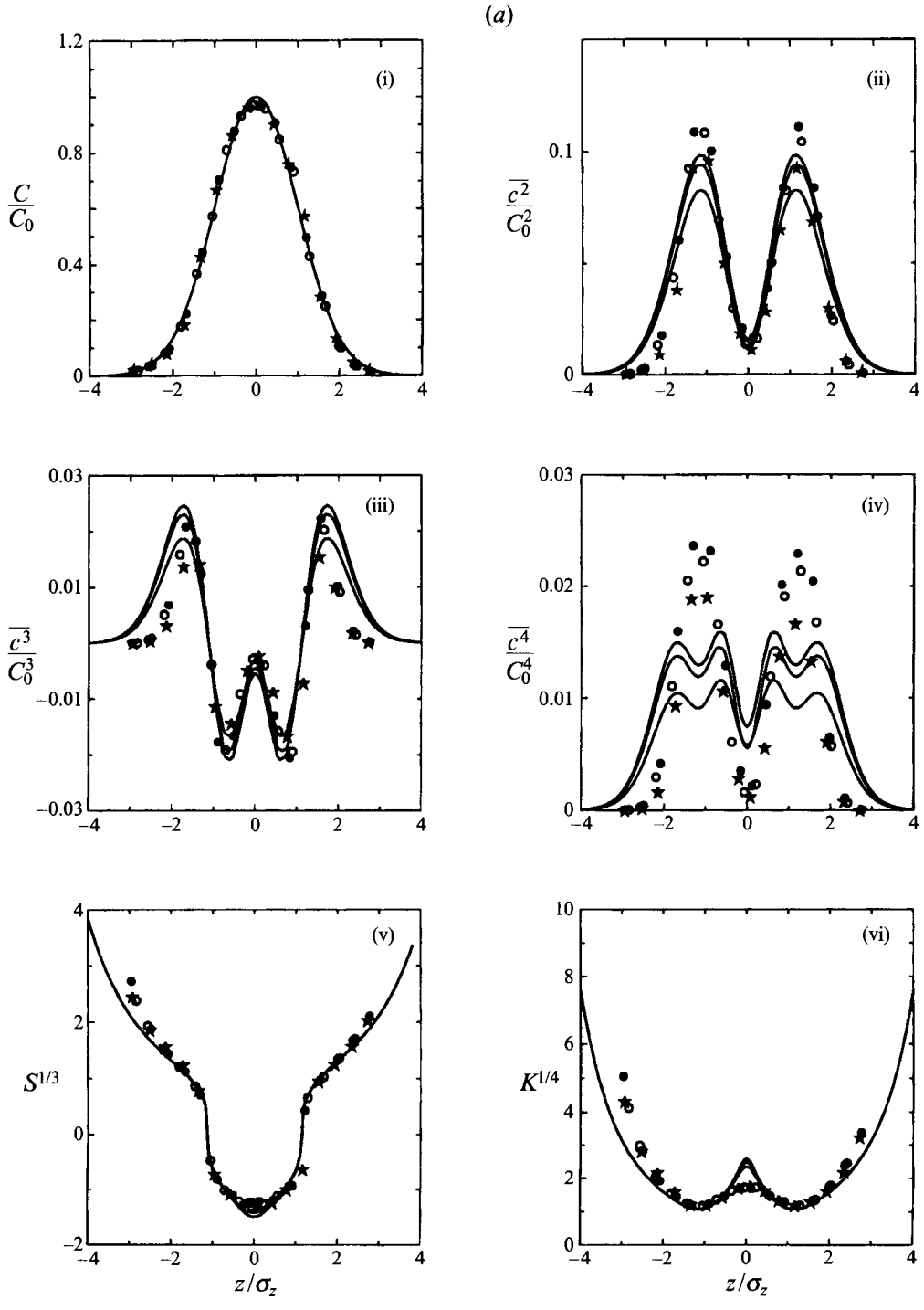

FIGURE 1(*a*). For caption see p. 147.

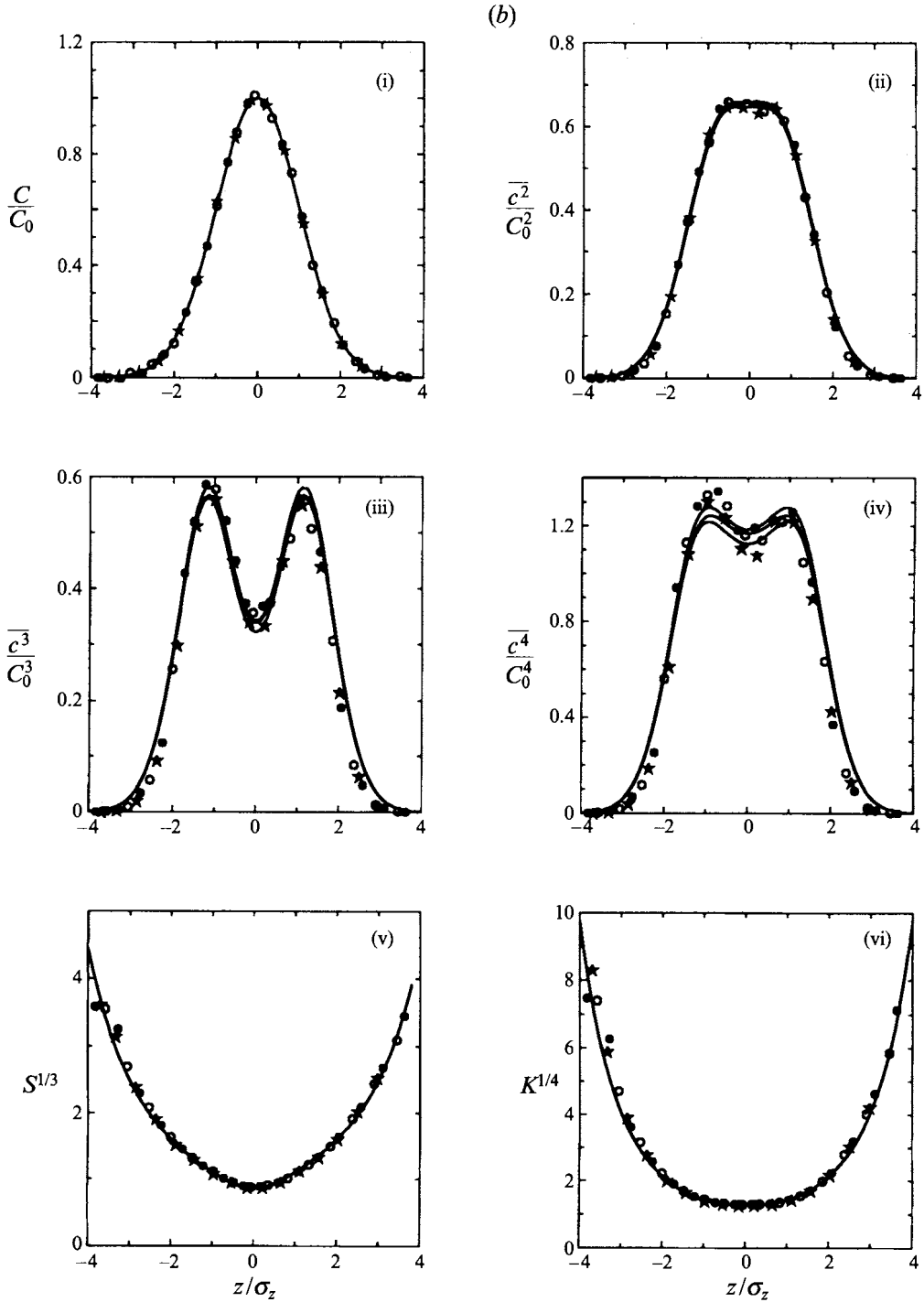

FIGURE 1(*b*). For caption see facing page.

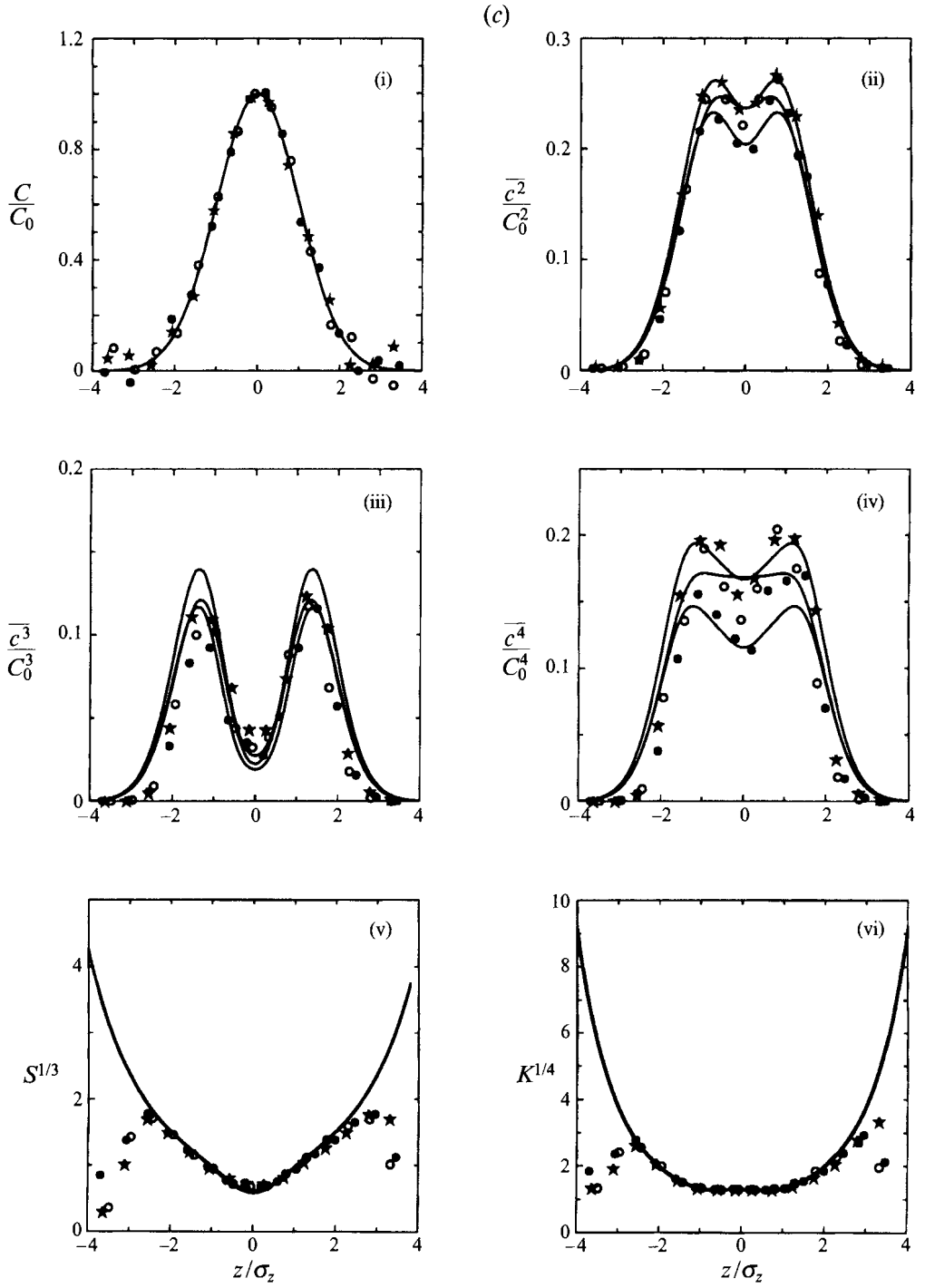

FIGURE 1. Cross-stream profiles for the mean (i), the second, third and fourth central moments, (ii)–(iv), the skewness (v) and kurtosis (vi) of the concentration field at downstream locations (*a*) $x/x_0 = 6.45 \times 10^{-3}$, (*b*) $x/x_0 = 0.323$ and (*c*) $x/x_0 = 8.39$. The points are from the data of Sawford & Tivendale (1992) for a line source in grid turbulence and the lines represent the best fit of the theory (12) to these data. Three replicates are shown.

2.2. *Representing the effects of molecular diffusion*

We are now in a position to complete the extension of Chatwin & Sullivan's theory for application to the developing scalar field downstream of an arbitrary, distributed source. In parallel with (4) concentration scales appropriate to a distributed source are introduced by replacing θ_0 in (10) with αC_0 and using the factor β^n, as in (4), to account for background concentrations due to κ. Here the additional parameters λ_n are in a form to distinguish between a uniform and non-uniform source. Note that although these new parameters are identified in terms of the integrals (11) over the source distribution, these results are strictly valid for $\kappa = 0$ and so in practice cannot be used to calculate the new parameters when $\kappa \neq 0$. Rather, following the philosophy of the original Chatwin & Sullivan approach, these results suggest an underlying structure which can be modified in an heuristic way to account for the effects of molecular diffusion. Thus α, β and λ_n will be determined empirically and will in general be functions of time in the case of a cloud or distance downstream in the case of a steady source. With these changes (10) becomes

$$\left.\begin{aligned} \overline{c^2}(\boldsymbol{x}, t) &= \beta^2 C_0^2 \chi(\alpha - \chi), \\ \overline{c^3}(\boldsymbol{x}, t) &= \beta^3 C_0^3 \chi(\lambda_3^2 \alpha^2 - 3\alpha\chi + 2\chi^2), \\ \overline{c^4}(\boldsymbol{x}, t) &= \beta^4 C_0^4 \chi(\lambda_4 \alpha^3 - 4\lambda_3^2 \alpha^2 \chi + 6\alpha\chi^2 - 3\chi^3), \\ &\vdots \end{aligned}\right\} \tag{12}$$

where for clarity of presentation the arguments of the functions have been suppressed. Of course, for $\lambda_n = 1$ and α and β constant, (4) is recovered from (12). It now remains to compare (12) with experimental data.

2.3. *The small-time behaviour of α and β*

Since it requires a finite time before the effects of molecular diffusion are significant, the results (4), (6) and (10) for $\kappa = 0$ apply as $t \to 0$, but the details depend on the nature of the source.

For a uniform source, comparison of (4) and (6) suggests that $\alpha(t) \sim \theta_0 / C_0(t)$ and $\beta(t) \sim 1$. This is also true for a steady source such as a jet or wake, for example, with time t replaced by distance downstream. Chatwin & Sullivan (1990) have shown that this statement has the interesting consequence that the cross-stream profile of the second moment will change from an initially bimodal distribution (for $\alpha(t) < 2$) to a unimodal distribution at larger times (or further downstream) where $\alpha(t) \geqslant 2$. This behavour is often observed experimentally and is apparent in figure 1 and also in figure 2. This small-time asymptotic behaviour provides a convenient and valuable reference base with which to assess the effects of molecular diffusion using experimental data.

We have shown that when the source is non-uniform the uniform source result for α and β will ultimately be reached when $\sigma_p(t) \gg L_0$. However, we indicated in the Introduction that experimental data do not conform to the uniform source result $\beta \to 1$ as $t \to 0$. The need to account for the details of the source distribution at small times is our main motivation for studying the non-uniform source case here and for contrasting it with results for a uniform source.

As a specific illustration which is germane to the interpretation of the experimental results presented in §3, consider an instantaneous, one-dimensional source in homogeneous turbulence. In this case the displacement probability density function is Gaussian,

$$P(z'; z, t) = \frac{1}{(2\pi)^{1/2} \sigma_p(t)} \exp\left(-\frac{(z - z')^2}{2\sigma_p^2(t)} \right), \tag{13}$$

where we recall that σ_p is the standard deviation of the displacement of independent particles released at a point.

For a uniform source distribution of concentration θ_0 on $|z| < L_0$,

$$C(z,t) = \theta_0 \pi(z,t) = \tfrac{1}{2}\theta_0 \left[\operatorname{erf}\left(\frac{L_0+z}{\sqrt{2}\sigma_p}\right) + \operatorname{erf}\left(\frac{L_0-z}{\sqrt{2}\sigma_p}\right)\right], \tag{14}$$

which, with (6), completely specifies the concentration moments. The function $\alpha(t)$ is

$$\alpha(t) = \theta_0 / C(0,t) = 1/\operatorname{erf}\left(\frac{L_0}{\sqrt{2}\sigma_p}\right), \tag{15}$$

which approaches unity as $t \to 0$ (i.e. at the source) and $\beta = 1$ (cf. (4)).

In contrast, we also consider the Gaussian area source distribution,

$$\mathscr{S}(x) = \sqrt{2}\theta_0 \exp\left(-\frac{z^2}{2\sigma_0^2}\right), \tag{16}$$

where a $\sqrt{2}$ is included, without loss of generality, so that from (11) $\lambda_2 = 1$. Using (16), (13) and (7), the nth moment of the concentration for $\kappa = 0$ is

$$\overline{\Gamma^n}(z,t) = \int_0^\infty \theta^n p(\theta; z, t)\, \mathrm{d}\theta = \frac{2^{n/2}\theta_0^n}{(1+n\hat{\sigma}^2(t))^{1/2}} \exp\left[-\frac{nz^2}{2\sigma_0^2(1+n\hat{\sigma}^2(t))}\right], \tag{17}$$

where $\hat{\sigma} = \sigma_p/\sigma_0$. The second central moment is

$$\overline{c^2}(z,t) = \overline{\Gamma^2}(z,t) - C^2(z,t). \tag{18}$$

The limit $\hat{\sigma}(t) \gg 1$ has already been discussed and then (17) reverts to (10) and, by comparison with (4), to the uniform source result $\alpha(t) = \theta_0/C_0(t)$ and $\beta = 1$. At smaller times the α, β structure of (4) only approximately represents the variance for a Gaussian source (i.e. (18) with C and $\overline{\Gamma^2}$ given by (17)). One way this approximation can be demonstrated is by matching the location and magnitude of the off-axis maximum value of the variance with that of (4). This procedure results in

$$\alpha(t) = 2\left(\frac{(1+\hat{\sigma}^2(t))^2}{(1+2\hat{\sigma}^2(t))^{3/2}}\right)^{(1+2\hat{\sigma}^2(t))/(2\hat{\sigma}^2(t))} \tag{19}$$

$$\beta^2(t) = \frac{1+2\hat{\sigma}^2(t)}{1+\hat{\sigma}^2(t)} - 1. \tag{20}$$

Again, for $\hat{\sigma}(t) \gg 1$ (19) and (20) give $\alpha(t) = \theta_0/C_0$ and $\beta(t) = 1$ respectively. As $t \to 0$, $\alpha(t) \to 2/\mathrm{e}^{1/2}$ and $\beta \to 0$. The approximation

$$\overline{c^2}(z,t) = C(z,t)\beta^2(t)(\alpha(t)\, C_0(t) - C(z,t)) \tag{21}$$

with $\alpha(t)$ and $\beta(t)$ given by (19) and (20) thus represents the salient features of the Gaussian source for both $t \to 0$ and for $\hat{\sigma}(t) \gg 1$ (which encompasses the transition from a bimodal to a unimodal distribution), as shown in figure 2. The feature to note in (20) is that, in contrast to the uniform source case, $\beta(t)$ monotonically increases from its initial value of zero.

It is straightforward to calculate explicitly the nth moment of the concentration for

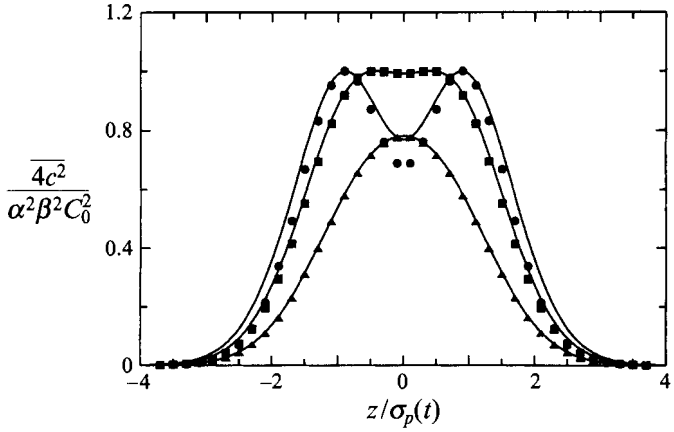

FIGURE 2. Cross-stream profiles of the concentration variance for a Gaussian source in the absence of molecular diffusion. The symbols represent (17) and (18) for $\hat{\sigma} = 1$ (●), $\hat{\sigma} = 2$ (■) and $\hat{\sigma} = 5$ (▲). The lines represent the theory (19), (20) and (12) with $(\alpha, \beta) = (1.35, 0.5)$, $(1.83, 0.8)$ and $(3.75, 0.96)$ respectively. The abscissa has been normalized by the particle dispersion, $\sigma_p(t)$ and C_0 is the centreline value of the mean concentration.

even more general sources in this special case of $\kappa = 0$ in homogeneous turbulence. The resulting near-source behaviour depends critically on the details of the source distribution. Consider for example the 'two-source problem' consisting of a pair of sources each of radius L_0 and separation d. In this case the cross-wind distribution of the concentration variance very near the source has four peaks corresponding to fluctuations generated by the large gradients near the edges of each source. Clearly such a complex structure is beyond the simple α, β description. However, even in this case, for travel times (or distances downstream) such that the single-particle dispersion is much larger than both L_0 and d, then the asymptotic result (10) holds.

3. Comparison with wind tunnel data

3.1. *Experimental details*

Here we make detailed comparisons between the theory and measured moments of the concentration field downstream of a line source in grid turbulence (Sawford & Tivendale 1992). The measurements were conducted in a suction wind tunnel with a rectangular test section 0.69 m high, 1.07 m wide and 3.3 m long. The turbulence was generated with a planar 'punched plate' grid with circular holes of diameter 0.0208 m in a hexagonal pattern, and 'mesh' length (i.e. hole spacing) $M = 2.54 \times 10^{-2}$ m, giving a solidity ratio of 0.39. Temperature fluctuations were produced by a heated Nichrome wire of diameter $d = 0.213$ mm placed a distance $x_0 = 12.2M$ downstream of the grid and spanwise across the tunnel. The experiments were carried out with a mean air speed $U = 5.0$ m s^{-1}. The Reynolds number, $Re = UM/\nu$, was 8500 where ν is the kinematic viscosity of unheated air (1.5×10^{-5} m^2 s^{-1} at 20 °C). The power supplied to the wire was 200 W m^{-1}, sufficient to eliminate vortex shedding.

Temperature fluctuations were measured with a 50 Ω platinum cold wire 1.27 μm in diameter and 0.4 mm long using an in-house-designed temperature bridge.

Cross-stream traverses of the plume were carried out using a screw-driven probe carriage. The cross-stream location of the probe was determined in relative terms to

0.01 mm. Traverses were carried out at approximately logarithmically spaced locations from 2 mm to 3 m downstream of the source.

The temperature signal was low-pass filtered at 2 kHz and sampled at 4096 Hz. Statistics were calculated from 20 separate 1 s samples, i.e. from a total of 81920 points. Temperature variance spectra indicated that frequencies up to 1 kHz account for 90% of the temperature variance at locations very near the source and over 99% of the variance far downstream. Our measurements, and the conclusions we draw here, are thus not strongly affected by instrumental averaging.

At the beginning and end of each set of 20 samples, 'background' samples were taken with the source wire switched off and after approximately 30 s stabilization time. The trend in these background readings was used as a first estimate of the baseline relative to which the mean temperature is calculated. However, it was found that the true baseline temperature (estimated by inspection of the time series) is higher. This was probably due to the effect of heating of the probe stubs and supports since the baseline offset was found to be proportional to the measured mean temperature in the plume and a correction was made for this effect.

3.2. *Results*

At all locations downstream of the source, the mean concentration profile for the data is indistinguishable from Gaussian. The function χ is therefore taken to be Gaussian. The first step in our analysis procedure is therefore to determine C_0 and a lengthscale (the mean plume dispersion, σ_z) defining the Gaussian function χ by a least-squares fit to the mean concentration data at a particular downstream location. We then fit the theory (12) to data for successively higher-order moments in turn, again using least-squares. The fit to $\overline{c^2}$ yields values for α and β which are then used in the fit to $\overline{c^3}$ in order to determine λ_3 and so on.

The above procedure was undertaken at 17 locations downstream of the source. In figure 1 fitted profiles are compared with the observations for the first four moments and also the skewness and kurtosis at three downstream locations: $x/x_0 = 6.45 \times 10^{-3}$ representative of the very near field, $x/x_0 = 0.323$ representative of the mid-field and $x/x_0 = 8.39$ which is representative of the far field. Different symbols for data points on figure 1 denote replications of the experiment, each of which has been independently fitted by the theory in order to indicate the experimental uncertainty in the process.

In general the original Chatwin & Sullivan theory gives a remarkably good fit to the data for the fluctuation field (i.e. the second moment) provided α and β are allowed to be slowly varying functions of distance downstream. Further, when shape factors λ_3 and λ_4 (which are also slowly varying functions of downstream distance) appropriate to a non-uniform source are used, a very good fit is obtained to the data for the distributed third and fourth central moments, given the inevitable experimental scatter to be expected in these demanding measurements.

In the near field the theory represents the first three moments well, particularly the location and magnitude of local extreme values, but does not represent the fourth moment at all well. The structure of the moments shown in figure 1(*a*) is typical of locations up to distances $x/x_0 = 3.23 \times 10^{-2}$ from the source, although over that range the local maximum in the third moment on the centreline gradually disappears, the centreline minimum in the even moments weakens and the fit to the fourth moment improves. There is a significant region near the centreline where the skewness is negative.

In the mid-field the theory represents all four moments very well. The significant changes in the structure are that the off-centreline maxima disappear from the second

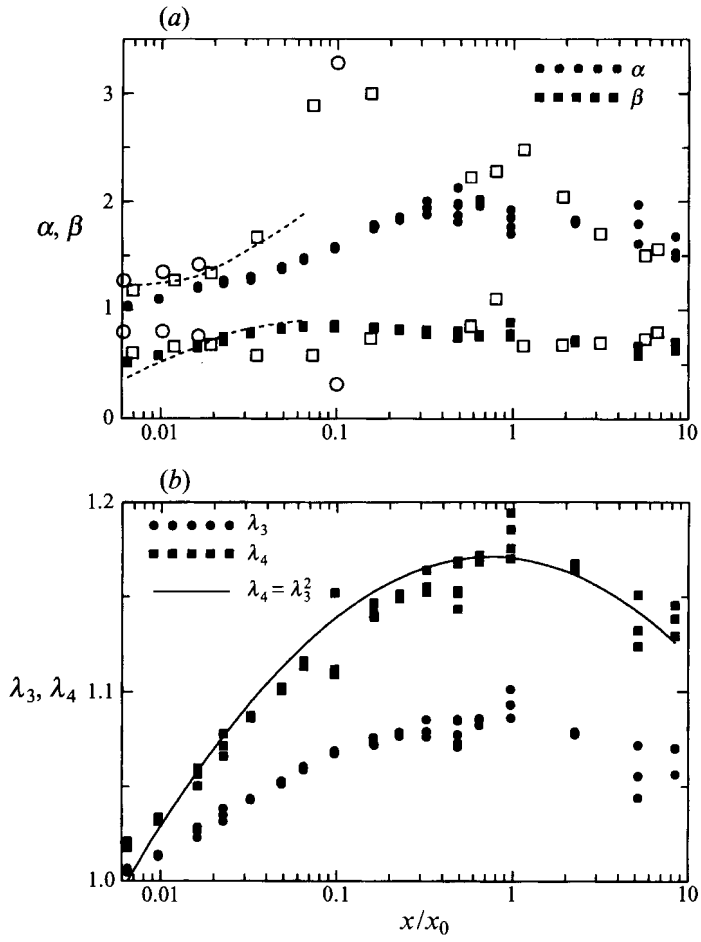

FIGURE 3. Best-fit values of the parameters (*a*) α and β, and (*b*) λ_3 and λ_4 as functions of downstream distance. The filled symbols represent fits to the data of Sawford & Tivendale (1992) as indicated in the legends. The open symbols in (*a*) represent fits to the data of Stapountzis *et al.* (1986) (○) and Warhaft (1984) (□) by Mosely (1991). The dashed lines in (*a*) represent the $\kappa = 0$ limit for a Gaussian source, calculated from (19) and (20) using measured values of $\hat{\sigma}(t)$ (see table 1).

moment, corresponding to values of $\alpha \approx 2$ in the theory (Chatwin & Sullivan 1990), and that the centreline value of the skewness changes sign to positive.

Finally, in the far field as shown in figure 1(*c*) the off-axis peaks in the second moment reappear weakly, corresponding to values of $\alpha < 2$. Although there is significant noise in the data at this location the theory still represents the data well. The overall features of the distributions correspond to the original Chatwin & Sullivan (1990) theory that is given in (4). However, it must be emphasized that the solid lines in figure 1 are derived from (12) where, at a given experimental station, a different value of λ_n is introduced for the fit to each of the higher moments.

The best-fit parameters for the theory are shown in figure 3 as functions of distance downstream from the source. Figure 3(*a*) shows α and β which are the fundamental parameters of the original theory and which are determined solely by the concentration mean and variance profiles. Values of α and β extracted by Moseley (1991) from the data of Stapountzis *et al.* (1986) and Warhaft (1984) are also shown in figure 3(*a*). These values are broadly consistent with the present results, but exhibit considerably

x/x_0	σ_z (mm)	σ_0^2 (mm^2)	$1+\hat{\sigma}^2$	i	$S^{1/3}$	$K^{1/4}$	α	β
6.45×10^{-3}	0.29	0.068	1.24	0.14	−1.23	1.62	1.23	0.44
9.68×10^{-3}	0.35	0.082	1.49	0.24	−1.11	1.44	1.26	0.57
1.61×10^{-2}	0.46	0.110	1.92	0.37	−0.96	1.28	1.34	0.69
2.26×10^{-2}	0.59	0.138	2.52	0.50	−0.80	1.18	1.44	0.77
3.23×10^{-2}	0.79	0.180	3.47	0.65	−0.54	1.11	1.60	0.84
4.84×10^{-2}	1.07	0.250	4.58	0.78	0.48	1.10	1.78	0.89
6.45×10^{-2}	1.33	0.320	5.53	0.86	0.65	1.11	1.91	0.91

TABLE 1. Centreline values of normalized concentration moments (the intensity, $i^2 = \overline{c^2}/C_0^2$, skewness, $S = \overline{c^3}/i^2C_0^3$ and the kurtosis, $K = \overline{c^4}/i^2C_0^4$), and fit parameters α and β, in the $\kappa = 0$ limit for a Gaussian source in homogeneous turbulence. The moments are calculated from (17) and the fit parameters from (19) and (20). The plume dispersion, σ_z, is taken directly from the measurements of Sawford & Tivendale (1992). The source size is corrected for diffusive growth of the instantaneous plume; namely $\sigma_0^2 = a_0 + 2\kappa x/U$, where $a_0 = 0.04$ mm^2, $\kappa = 0.35$ cm^2 s^{-1} and $U = 5$ m s^{-1}. The lengthscale $x_0 = 310$ mm.

more scatter. In the near field α and β follow the predictions for the $\kappa = 0$, Gaussian source example of (19) and (20), which are shown as the dashed lines in figure 3(*a*). In evaluating (19) and (20), measured values of the plume dispersion were used. Because the source wire is so small for the data reported in figure 3(*a*), the instantaneous plume initially grows by molecular diffusion alone until it is large enough to be affected by the smallest turbulent eddies. The effective source size was therefore approximated by the sum of a constant term representing the size of the source wire and its boundary layer and a purely diffusive growth term, viz. $\sigma_0^2 = a_0 + 2\kappa x/U$. The molecular diffusivity was taken to be 0.35 cm^2 s^{-1} corresponding to a plume temperature of about 150 °C, and the wind speed was 5 m s^{-1}. The constant term was taken to be 0.04 mm^2 in order to match the predicted and measured intensity of concentration fluctuations (see figure 4(*a*)) at the measurement point nearest the source. These calculations are summarized in table 1. Although there is necessarily a degree of empiricism in these calculations, the agreement with the measured values of α and β suggests that the physical picture underlying (19) and (20) is correct at small distances from the source. At about $x/x_0 = 0.5$, α reaches a maximum of about 2 corresponding, as noted earlier, to the disappearance of off-axis peaks in the variance profile. Further downstream α decreases steadily due to the interaction of molecular diffusion and the convective effects of the turbulence. With increasing distance downstream β also departs from the $\kappa = 0$ theory, reaching a maximum at $x/x_0 \approx 0.06$ and then decreasing steadily. There is no apparent sign of an approach to constant values of α and β, which would indicate self-similarity of the scalar field, far downstream.

The shape factors λ_3 and λ_4 are shown in figure 3(*b*); they represent scaling factors for α, due to a non-uniform source, in the theory for the third and fourth moments as indicated in (12). The original theory for a uniform source (4) corresponds to $\lambda_3 = \lambda_4 = 1$, but these values do not give an adequate representation of the third and fourth moments. For example, for the present experimental data where $\alpha \leqslant 2$ (see figure 3*a*), the centreline skewness is positive for $x/x_0 > 0.6$ (figure 4*b*), but the original theory predicts the centreline skewness to be negative (see Chatwin & Sullivan 1990, figure 6*d*).

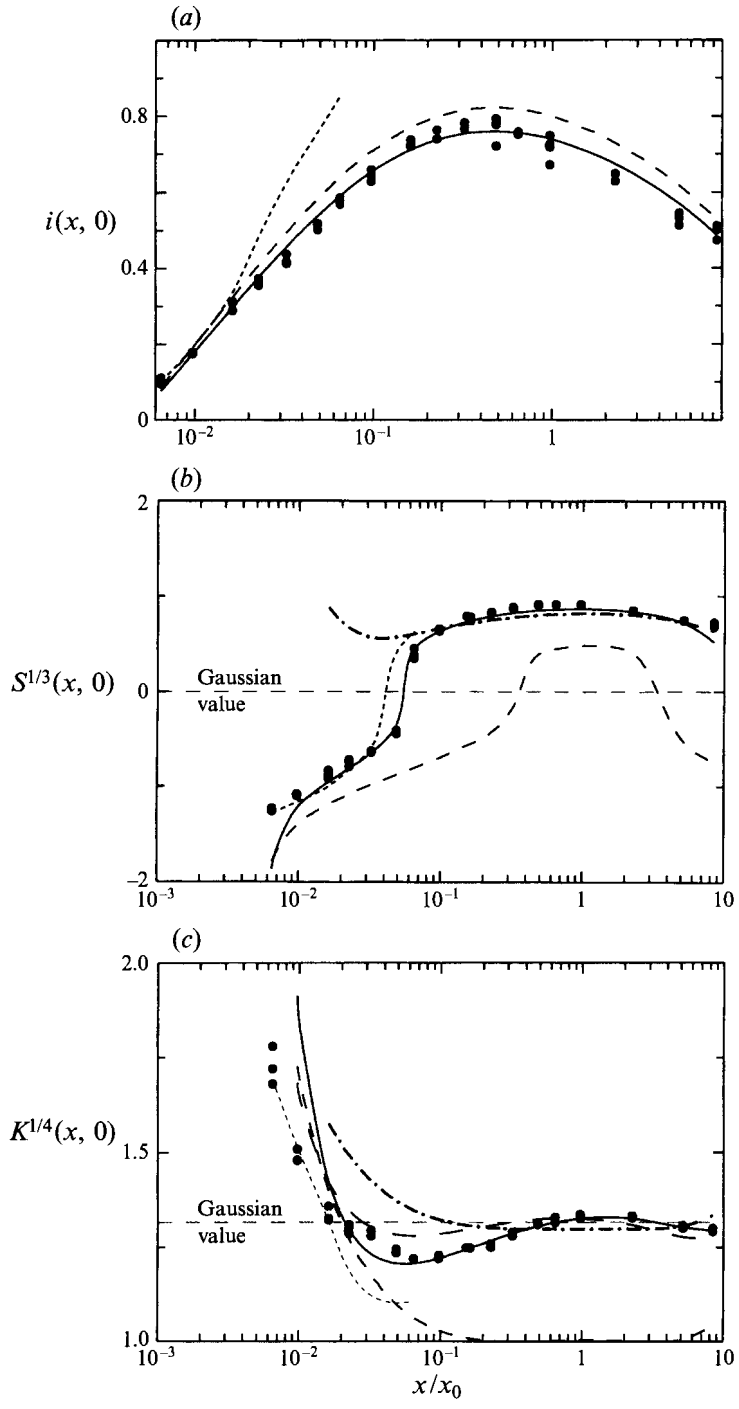

FIGURE 4. Centreline values of (*a*) the intensity of concentration fluctuations, (*b*) the skewness and (*c*) the kurtosis as functions of downstream distance. The points are the data of Sawford & Tivendale (1992). The lines are the theory (12) (——); the theory (12) with $\lambda_2 = \lambda_3 = \lambda_4 = \bar{\lambda}$ (---); with $\lambda_4 = \lambda_3^2$ (– –) (for (*c*) only); with $\lambda_3 = 1.07$ and $\lambda_4 = 1.15$ (– · – · –), and the $\kappa = 0$ limit (17) for a Gaussian source (see table 1), (· · · · · ·).

3.3. *Sensitivity analysis*

The variation in the shape factors is not strong (less than 10% and 20% for λ_3 and λ_4 respectively), so it is of interest to test the sensitivity of predictions of the moments to simple approximations to the shape parameters.

A reasonable approximation for λ_4 in terms of λ_3 can be obtained from the hypothesis that the ratio λ_{n+1}/λ_n is a slowly varing function of n. By definition, $\lambda_3/\lambda_2 = \lambda_3$ so $\lambda_4/\lambda_3 \approx \lambda_3$ results in

$$\lambda_4(x) \approx \lambda_3^2(x). \tag{22}$$

The values of λ_4 calculated from (22), using the average values of λ_3, are given by the solid line in figure 3(*b*) and are in good agreement with the measured values of $\lambda_4(x)$ throughout the experimental range. To this degree of approximation the distributed moments can be represented by the three functions $\alpha(x)$, $\beta(x)$ and $\lambda_3(x)$.

In practical applications interest is mostly focused on the centre of the plume where concentrations are highest. In figure 4 we compare predictions of the centreline values of the normalized moments (the intensity, $i^2 = \overline{c^2}/C_0^2$, skewness, $S = \overline{c^3}/i^2C_0^3$ and the kurtosis, $K = \overline{c^4}/i^2C_0^4$) with the measurements. The full theory is shown as the solid line in each of figures 4(*a*), 4(*b*) and 4(*c*). The $\kappa = 0$ limit (17) for a Gaussian source is also shown.

Although the theory is capable of providing a good representation of most of the data over the whole range of downstream locations, four separate functions of distance are needed to do so. Accordingly, we also show in figure 4 three approximations to the full theory which are less demanding in their data requirements.

The first of these uses a single function to represent all of the λ_n for $n = 2$, 3 and 4; we simply use the mean $\bar{\lambda} = (\lambda_2+\lambda_3+\lambda_4)/3$, where we recall that $\lambda_2 = 1$ by definition. Since the λ always occur in combination with α, this approximation is equivalent to using only two functions, $\bar{\lambda}\alpha$ and β, to represent all three moments. It overestimates the intensity of fluctuations by a few percent but otherwise follows the trend very well. However, it provides only a tolerable representation of the skewness and kurtosis in the near field ($x/x_0 < 0.04$) and is quite poor in the far field.

With the approximation (22), the intensity and skewness are unchanged from the full theory, and the downstream dependence of the kurtosis is represented almost as well as the full theory.

Finally, we see from figures 4(*b*) and 4(*c*) that constant values of the shape factors ($\lambda_3 = 1.07$; $\lambda_4 = 1.15$) represent the centreline skewness and kurtosis well in the far field.

We conclude that although the variation of the shape factors is not large it is nevertheless significant in accurately predicting the magnitude of the moments and hence a probability density function derived by inverting these moements.

4. Conclusions

For the special case of homogeneous turbulence we have examined the Chatwin & Sullivan (1990) theory using some simple theoretical results and a detailed experimental data set. In particular we have explored the effect of relaxing the assumption of a uniform source distribution and of allowing the parameters in the theory to be functions of downstream distance.

The downstream domain can be divided into two regions: a near field where turbulent dispersion is small compared with the source lengthscale and where details

of the source distribution are important, and a far field where only broad features of the source are important.

In the near field the structure of moments of the concentration field depends sensitively on the source distribution. The Chatwin & Sullivan theory does not, and cannot be expected to, reproduce this structure for complex source distributions such as multiple sources. However, even for single sources we show that in the near field the structure of concentration statistics is sensitive to the source distribution. In this case however, the α, β theory is capable of representing the structure of the second moment, but with different values of α and β for different sources. For a uniform source $\beta \to 1$ at the source, whereas a best-fit β for a Gaussian source approaches zero at the source. Thus we are able to explain the experimentally observed behaviour of β at small times in terms of departures from a uniform source distribution.

In the far field we find through theoretical analysis that the spatial structure of the second moment is independent of the source distribution, although the values of the parameters α and β may still depend on the source details. In general however, the structure of each higher moment involves an additional parameter. Although these new parameters are identified in terms of integrals over the source distribution, these results are strictly valid for $\kappa = 0$ and so in practice cannot be used to calculate the new parameters when $\kappa \neq 0$. Rather, following the philosophy of the original Chatwin & Sullivan approach, these results suggest an underlying structure which can be modified in an heuristic way to account for the effects of molecular diffusion. The significance of the new results presented here is that they show that in general this underlying structure is more complicated than that in the original theory, but that this is only manifested in moments higher than the second.

The extended theory gives a good representation of the first four moments of the concentration field downstream of a line source of heat in grid turbulence everywhere except for the higher moments very near the source. The asymptotic, self-similar, scalar field addressed in Chatwin & Sullivan (1990) is not clearly reached with these experimental data, and the small but significant differences in the shape factors, associated with the non-uniform source, do persist to the furthest measuring station downstream.

The requirement to represent the behaviour of the first four moments of the concentration field over the whole downstream domain is very demanding and is unlikely to be met in detail by simple models such as those discussed here without the extensive parameterization inherent in the specification of the functions α and β and the shape factors. We have shown that some extension of the original theory is necessary (to get the right sign of the centreline skewness for example) but the requirements in practice are unlikely to be as demanding. For example, constant values of the shape factors work well in the far field. How broadly these simple results apply to other flow configurations will only be answered through detailed measurements and comparisons of the sort undertaken here.

This work has received financial support from the National Science and Engineering Research Council of Canada. It is a pleasure to acknowledge illuminating discussions and correspondence with Philip Chatwin and Nils Mole, and the thoroughness and ingenuity of Charles Tivendale in making the measurements.

REFERENCES

CHATWIN, P. C. & SULLIVAN, P. J. 1979 The relative diffusion of a cloud of passive contaminant in incompressible turbulent flow. *J. Fluid Mech.* **91**, 337–355.

CHATWIN, P. C. & SULLIVAN, P. J. 1987 Perceived statistical properties of scalars in turbulent shear flows. In *Proc. 6th Symp. on Turbulent Shear Flow, Toulouse France*, pp. 9.1.1–9.1.6.

CHATWIN, P. C. & SULLIVAN, P. J. 1989 The intermittency factor of scalars in turbulence. *Phys. Fluids* A **1**, 761–763.

CHATWIN, P. C. & SULLIVAN, P. J. 1990 A simple and unifying physical interpretation of scalar fluctuation measurements from many turbulent shear flows. *J. Fluid Mech.* **212**, 533–556.

CHATWIN, P. C. & SULLIVAN, P. J. 1993 The structure and magnitude of concentration fluctuations. *Boundary Layer Met.* **62**, 169–280.

CHATWIN, P. C., SULLIVAN, P. J. & YIP, H. 1990 Dilution and marked fluid particle analysis. In *Proc. Intl. Conf. on Physical Modelling of Transport and Dispersion* (ed. E. E. Adams & G. E. Hecker), pp. 6B3–6D8. Massachusetts Inst. of Tech.

DERKSEN, R. W. & SULLIVAN, P. J. 1990 Moment approximations for probability density functions. *Combust. Flame* **81**, 378–391.

DERKSEN, R. W., SULLIVAN, P. J. & YIP, H. 1994 Asymptotic probability density function of a scalar. *AIAA. J.* **31**, 1083–1084.

FACKRELL, J. E. & ROBINS, A. G. 1982 Concentration fluctuations and fluxes in plumes from point sources in a turbulent boundary layer. *J. Fluid Mech.* **117**, 1–26.

KARNIK, V. & TAVOULARIS, S. 1989 Measurements of heat diffusion from a continuous line source in a uniformly sheared turbulent flow. *J. Fluid Mech.* **20**, 233–261.

MOSELEY, D. J. 1991 A closure hypothesis for contaminant fluctuations in turbulent flow. MSc thesis, University of Western Ontario.

SAWFORD, B. L. & TIVENDALE, C. M. 1992 Measurements of concentration statistics downstream of a line source in grid turbulence. In *Proc. 11th Australasian Fluid Mechanics Conf., Hobart, Dec. 14–18, 1992*, pp. 945–948. University of Tasmania.

STAPOUNTZIS, H., SAWFORD, B. L., HUNT, J. C. R. & BRITTER, R. E. 1986 Structure of the temperature field downwind of a line source in grid turbulence. *J. Fluid Mech.* **65**, 401–424.

SULLIVAN, P. J. 1971 Some data on the distance-neighbour function for relative diffusion. *J. Fluid Mech.* **47**, 601–607.

SULLIVAN, P. J. & YIP, H. 1989 An approach for predicting some statistics relevant to contaminant spread in an atmospheric boundary layer. In Continuum Mechanics and Its Applications (ed. G. A. C. Graham & S. K. Malik), pp. 837–847. Hemispheric.

WARHAFT, Z. 1984 The interference of thermal fields from line sources in grid turbulence. *J. Fluid Mech.* **144**, 368–387.